

**Olefin Metathesis**

# Hydrogen Bonding Networks Enable Brønsted Acid-Catalyzed Carbonyl-Olefin Metathesis\*\*

Tuong Anh To, Chao Pei, Rene M. Koenigs,\* and Thanh Vinh Nguyen\*

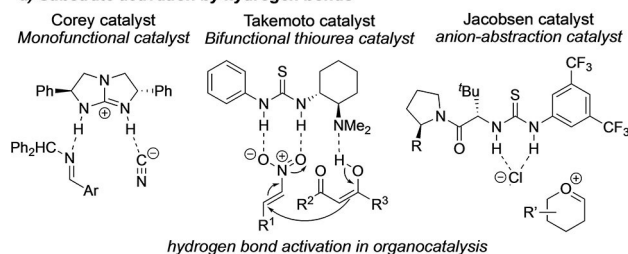
**Abstract:** Synthetic chemists have learned to mimic nature in using hydrogen bonds and other weak interactions to dictate the spatial arrangement of reaction substrates and to stabilize transition states to enable highly efficient and selective reactions. The activation of a catalyst molecule itself by hydrogen-bonding networks, in order to enhance its catalytic activity to achieve a desired reaction outcome, is less explored in organic synthesis, despite being a commonly found phenomenon in nature. Herein, we show our investigation into this underexplored area by studying the promotion of carbonyl-olefin metathesis reactions by hydrogen-bonding-assisted Brønsted acid catalysis, using hexafluoroisopropanol (HFIP) solvent in combination with *para*-toluenesulfonic acid (pTSA). Our experimental and computational mechanistic studies reveal not only an interesting role of HFIP solvent in assisting pTSA Brønsted acid catalyst, but also insightful knowledge about the current limitations of the carbonyl-olefin metathesis reaction.

## Introduction

Weak non-covalent interactions take up an essential role in chemistry and biology and form the basis for the assembly of complex supramolecular structures in natural and artificial systems.<sup>[1]</sup> Among them, the hydrogen bond is of unique importance and indispensable for the formation of entities

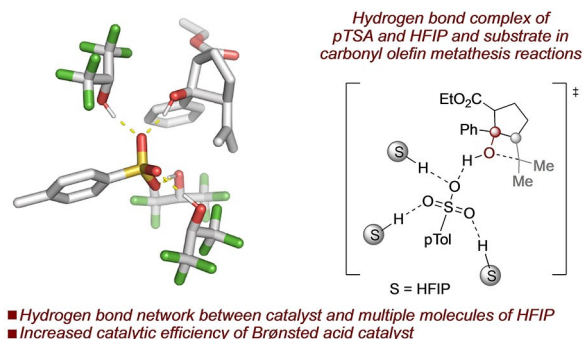
essential for living, such as proteins or nucleic acids.<sup>[2]</sup> Chemists often mimic nature in using hydrogen bonds to dictate the spatial arrangement of individual molecules in supramolecular assemblies<sup>[3]</sup> or to stabilize transition states in catalysis to enable highly efficient and selective reactions.<sup>[4]</sup> One of the longest standing paradigms in catalysis lies within the activation of reaction substrates with hydrogen-bonding catalysts, which also are small organic molecules themselves.<sup>[5]</sup> Numerous hydrogen-bonding motifs have been reported to date and the Corey, Schreiner or Takemoto catalysts (Scheme 1a) represent a few versatile and well-explored examples of such systems. Another well-established paradigm in this field was the anion-abstracting catalysis pioneered by Jacobsen and co-workers (Scheme 1a).<sup>[6]</sup> Nonetheless, the activation of a catalyst molecule itself by hydrogen bonds is relatively less explored in organic synthesis, despite being a common occurrence in biological chemistry.<sup>[2,4c]</sup> Some relevant systems reported in literature include the synergistic pTSA/HFIP hydrogen-bonding complexes for intramolecular hydroarylation of

### a) Substrate activation by hydrogen bonds



- Substrate activation via hydrogen bonds
- Preorganization of substrates via hydrogen bonds

### b) This work: Catalyst activation by hydrogen bonds



**Scheme 1.** Hydrogen-bonding complexation with solvent activates Brønsted acid catalysts for the promotion of otherwise challenging chemical transformation.

[\*] T. Anh To, Dr. T. Vinh Nguyen  
 School of Chemistry  
 University of New South Wales, Sydney  
 Anzac Parade, Kensington, NSW 2052 (Australia)  
 E-mail: t.v.nguyen@unsw.edu.au

C. Pei, Prof. Dr. R. M. Koenigs  
 Institute of Organic Chemistry  
 RWTH Aachen  
 Landoltweg 1, 52074 Aachen (Germany)  
 E-mail: rene.koenigs@rwth-aachen.de

[\*\*] A previous version of this manuscript has been deposited on a preprint server (<https://doi.org/10.33774/chemrxiv-2021-gpllr-v2>).

© 2022 The Authors. Angewandte Chemie International Edition published by Wiley-VCH GmbH. This is an open access article under the terms of the Creative Commons Attribution Non-Commercial NoDerivs License, which permits use and distribution in any medium, provided the original work is properly cited, the use is non-commercial and no modifications or adaptations are made.

alkynes by Ichikawa and co-workers,<sup>[7]</sup> or the tetrafluoro-terephthalic acid/HFIP hydrogen-bonding complexes for the coupling reaction of quinone monoacetals and alkenes by Kita and co-workers.<sup>[8]</sup> In both studies, relatively weak or mild Brønsted acids were activated by HFIP to become potent reaction promoters.

We believe that this strategy would be useful in frequently encountered synthetic scenarios where highly reactive catalysts are not only efficient for the desired chemical transformation but also promote unwanted side-reactions at the same time.<sup>[9]</sup> By employing a moderately or poorly active catalyst to ensure better selectivity, and enhancing its efficacy by hydrogen-bonding interactions, the overall outcome of the catalytic reaction can be improved. For this purpose, it is ideal for the reaction solvent to also act as the required hydrogen-bonding molecules.<sup>[4b]</sup> While there are many solvents capable of forming hydrogen bonds, with water being the one in biological systems, perfluorinated alcohols such as HFIP are attractive options for organic synthesis.<sup>[10]</sup> HFIP has been known to mediate a wide range of reactions as a highly ionizing solvent with excellent hydrogen-bonding capability, yet, its unique role in catalysis remains poorly understood.<sup>[11]</sup> Simple and mildly Brønsted acidic catalysts with multiple hydrogen-bond acceptor groups, such as carboxylic acids or sulfonic acids, could become suitable models to further explore the concept of catalyst activation by hydrogen-bonding networks.

To study such novel catalyst systems, we embarked on the investigation of their efficiency on the carbonyl-olefin metathesis (COM) reaction.<sup>[12]</sup> The COM reaction has been identified as an attractive replacement to overcome challenges in traditional approaches for the olefination of carbonyl groups, such as pre-functionalization of substrates, reagent synthesis, or the separation of by-products from reaction mixtures.<sup>[13]</sup> The majority of approaches towards COM reactions are based on Lewis acid catalysts,<sup>[14]</sup> ranging from transition metal salts such as FeCl<sub>3</sub> first reported by Schindler et al.<sup>[12c,15]</sup> and Li et al.<sup>[12d]</sup> and subsequently salts of Ga<sup>III</sup> by Schindler<sup>[16]</sup> and Bour,<sup>[12f]</sup> AuCl<sub>3</sub> by Lin et al.<sup>[17]</sup> or bimetallic systems such as AlCl<sub>3</sub>/AgSF<sub>6</sub> and AlCl<sub>3</sub>/AgSF<sub>6</sub> by Schindler.<sup>[18]</sup> Further, more specialized approaches harness the reactivity of hydrazines as organocatalysts as reported by the Lambert group<sup>[12a,19]</sup> and a special photocatalytic strategy by the Glorius group.<sup>[12e]</sup> There have also been notable applications of metal-free Lewis acids in promoting COM reactions such as the tritylium catalysts by Franzén and co-workers<sup>[12b,20]</sup> as well as tropylium salts<sup>[21]</sup> and iodonium ion<sup>[22]</sup> reported by our Nguyen group. Silylium or phosphonium-based Lewis acids also showed potential catalytic activity for COM reactions.<sup>[23]</sup> Despite recent advances in COM reactions with various Lewis acid catalysts,<sup>[13]</sup> the field is still in its infancy and a generalized approach towards Brønsted acid-catalyzed COM reactions remains elusive. Up to this date, there have been only two reports on efficient Brønsted acid catalyzed COM reactions, with both of them employing elegant but very specially designed systems using fixation of the acid catalyst in a supramolecular capsule by the Tiefenbacher group<sup>[24]</sup> or within a fixed-bed in continuous flow system by Layva-Pérez

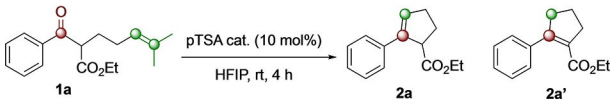
and co-workers.<sup>[25]</sup> Simple generalized methods towards COM reactions that can operate homogeneously in bulk solvent have not been reported thus far. Furthermore, the COM reaction is even more suitable for the investigation of our catalysis concept (Scheme 1b), considering the fact that previous attempts to use superacidic catalysts such as triflic acid to catalyze COM reaction often led to unsatisfactory or unwanted outcomes.<sup>[26]</sup>

## Results and Discussion

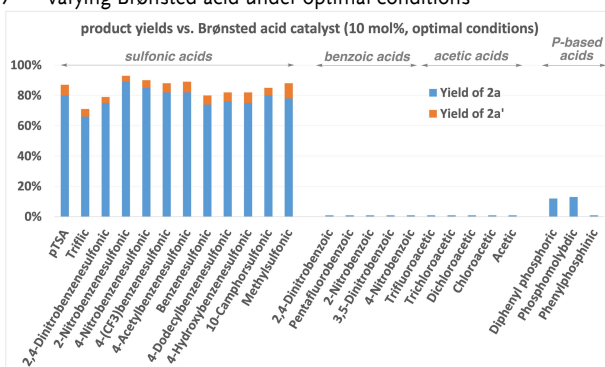
To probe our hypothesis on hydrogen-bond network-assisted, Brønsted acid-catalyzed COM reactions, we studied the influence of solvent on the reaction substrate **1a** using pTSA as a simple readily available Brønsted acid catalyst. Pleasingly, the reaction worked optimally with 10 mol% of pTSA catalyst in 100  $\mu$ L HFIP for the 0.2 mmol scale reaction, giving the product **2a** in 80 % yield after 4 hours at ambient temperature (entry 1, Table 1).<sup>[27]</sup> Solvents such as 1,2-dichloroethane (DCE), *i*PrOH or linear fluorinated alcohols, which are weaker hydrogen-bonding agents than HFIP, proved to be inefficient (entries 2–6, Table 1). <sup>1</sup>H NMR studies on the perturbation of the pTSA acidic proton signal in the presence of a varying amount of HFIP showed clear evidence of such a hydrogen-bonding network, and this effect was stronger with HFIP than *i*PrOH or TFE (see pages S4–S7 in the experimental Supporting Information for further details). The respective <sup>1</sup>H NMR studies on the interaction of HFIP with substrate **1a** showed no evidence on potential solvent-substrate interaction (see page S8 in the experimental Supporting Information).

Furthermore, the use of a squaramide or a thiourea catalyst as hydrogen-bonding donors did not lead to any productive outcomes either (entries 7 and 8), thus demonstrating the importance of HFIP and the formation of a strong hydrogen-bond network to enhance catalytic efficiency of pTSA and improve the efficiency of the COM reaction. In the absence of catalyst, no reaction was observed (entry 9) and lower catalyst loading was detrimental to the reaction efficiency (entry 10). Reducing the amount of HFIP led to lower efficiencies while using more HFIP resulted in comparable reaction outcomes (entries 11–13). Overall, the optimal conditions developed here are milder and more practical than previous reports on other Brønsted acid catalyzed COM systems, which used more complicated reaction setups, elevated temperatures and longer reaction times.<sup>[24,25]</sup>

It should be emphasized here that we also did a careful screening of a wide range of Brønsted acids (entry 17, Table 1, also see page S10 in the experimental Supporting Information for details). Interestingly, most sulfonic acids (acidic moiety containing three oxygens) can efficiently promote the COM reaction of substrate **1a** to a mixture of major product **2a** and its isomerized alkene **2a'**. All tested benzoic and acetic acids (acidic moiety containing two oxygens), including TFA, only led to traces amount of COM products, although some of them have comparable *pK<sub>a</sub>*s to those working sulfonic acids. Some phosphorus-based

**Table 1:** Optimization of the HFIP-promoted Brønsted acid-catalyzed COM.


Entry <sup>[a]</sup>	Variations from optimal conditions <sup>[b]</sup>	Yield of <b>2a</b> [%] <sup>[c]</sup>
1	none (HFIP = 100 $\mu$ L)	80
2	neat	n.p.
3	DCE instead of HFIP	n.p.
4	<sup>i</sup> PrOH instead of HFIP	n.p.
5	TFE (CF <sub>3</sub> CH <sub>2</sub> OH) instead of HFIP	15
6	CF <sub>3</sub> CF <sub>2</sub> CH <sub>2</sub> OH instead of HFIP	n.p.
7	catalyst <b>A</b> or <b>B</b> (10 mol%) instead of pTSA	n.p.
8	pTSA and catalyst <b>A</b> or <b>B</b> (10 mol%, instead of HFIP), in DCE	n.p.
9	absence of pTSA	n.p.
10	pTSA (5 mol%)	73
11	HFIP (50 $\mu$ L)	56
12	HFIP (75 $\mu$ L)	62
13	HFIP (200 $\mu$ L)	80
14	TfOH (10 mol%) instead of pTSA, in HFIP	66
15	TfOH (10 mol%) instead of pTSA, in DCE instead of HFIP	36
16	HCl (10 mol%) instead of pTSA, in HFIP	traces
17	varying Brønsted acid under optimal conditions	



[a] Reaction conditions: **1a** (0.2 mmol), pTSA (10 mol%), HFIP (100  $\mu$ L) at RT for 4 h. [b] For further details on optimization studies, see pages S9, S10 in the experimental Supporting Information. [c] Yield based on <sup>1</sup>H NMR integration using methyl benzoate as an internal standard, n.p. = no product.

Brønsted acids (acidic moiety containing two or four oxygens, except phosphomolybdic acid) gave positive but unsatisfactory reaction outcomes. HCl did not work under our optimal conditions. Considering overall product yield, level of isomerization and commercial availability, we decided to keep using pTSA as our Brønsted catalyst of choice. It should be noted here again that previous attempts using triflic acid to catalyze COM reactions often led to different or unsatisfactory outcomes,<sup>[26]</sup> especially in other solvent than HFIP as evidenced by entry 15 (Table 1).

For further understanding of the reaction mechanism and the role of HFIP and the hydrogen-bond network on the reaction, we carried out a series of kinetic studies with substrate **1a** and 5 mol% of pTSA in varying amount of HFIP from 2 to 6 equivalents with respect to **1a** in CDCl<sub>3</sub>

(Figure 1). The conversion of **1a** was monitored by <sup>1</sup>H NMR spectroscopy over time (see pages S12, S13 in the experimental Supporting Information for more details). The kinetic data for initial reactions rates after  $\approx 10\%$  conversions was analyzed and showed that the reaction order in HFIP was  $\approx 2.5$  (Figure 1), which suggested that only a small number of HFIP solvent molecules were directly involved in the rate determining step of the COM reaction under investigation.

To understand experimental reaction kinetics and to rationalize the influence of HFIP on the reaction mechanism, we next embarked on computational studies on the pTSA-catalyzed reaction of **1a** (Scheme 2). First, we examined an implicit solvent model for HFIP<sup>[28]</sup> that does not allow for interaction of solvent molecules with substrate and/or catalyst (Scheme 2a, grey energy profile). Second, we used a combination of explicit solvent molecules and an additional implicit solvent model. For this, we added varying amounts of explicit molecules of HFIP to the calculation to account for the formation and influence of a hydrogen-bond network between solvent molecules and catalyst (Scheme 2a, dark blue energy profile; for sampling of hydrogen-bond interactions, see Figure S22 in the computational Supporting Information for details).

Disregarding of the solvent model used, the calculations show that this COM reaction proceeds via the same elementary reaction steps and initiates via an intramolecular C–C bond formation reaction, followed by oxetane formation, ring opening and elimination reaction to provide olefin

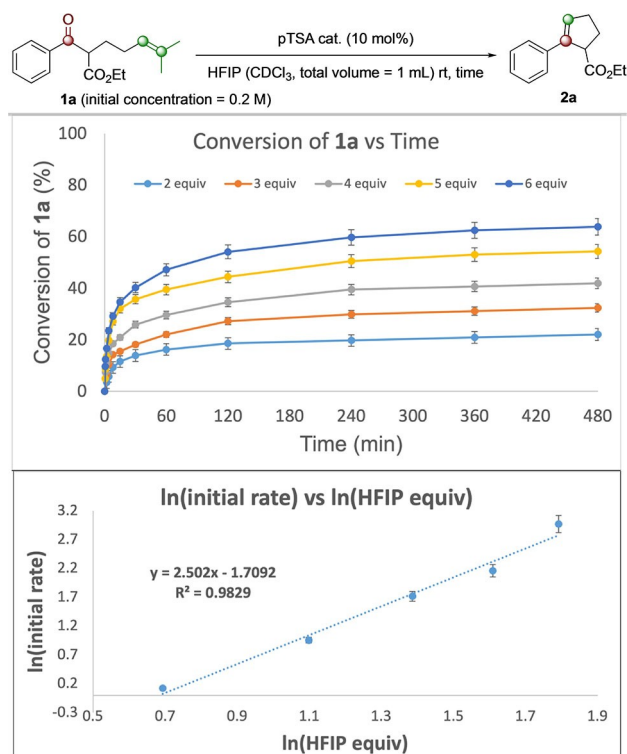
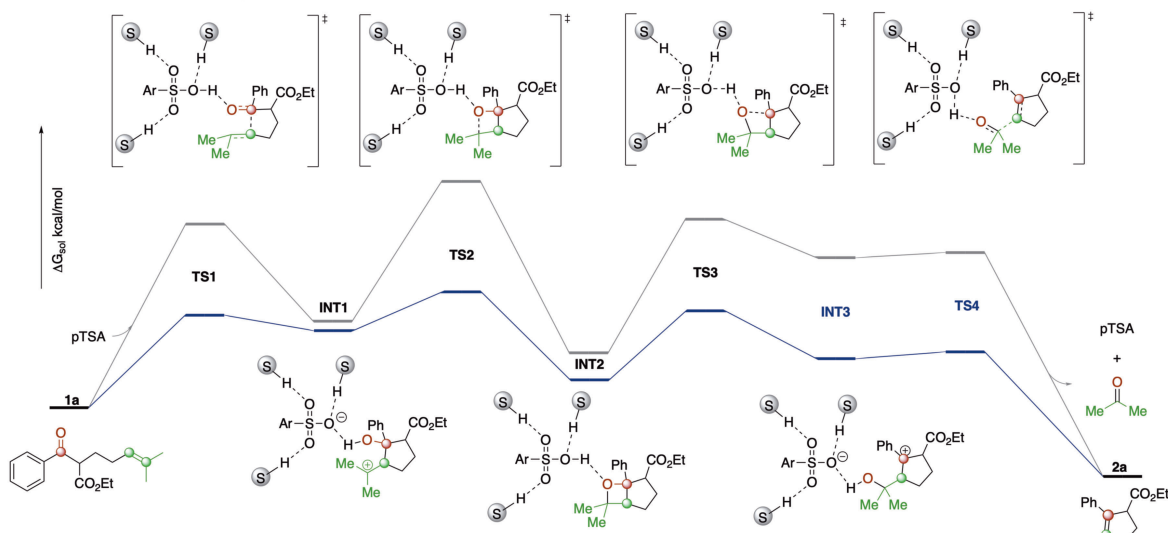


**Figure 1.** Kinetic studies of the conversion of **1a** to product **2a** with different amounts of HFIP. See pages S12 and S13 in the experimental Supporting Information for more details.

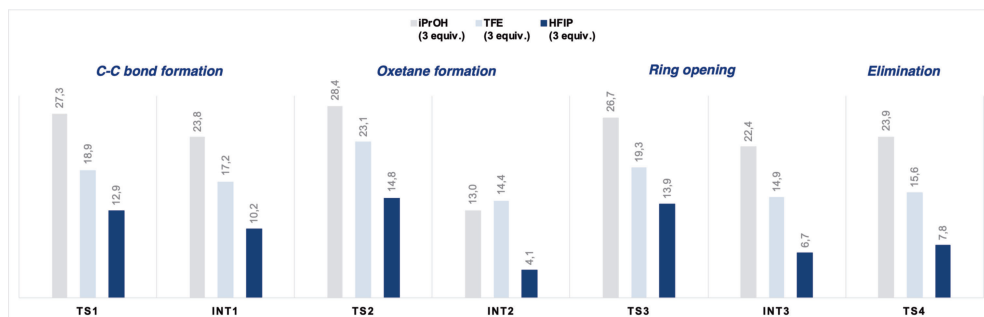
## a) Influence of hydrogen bond network on the reaction profile of the COM reaction

Evaluation of implicit solvent model for HFIP (grey) and a combined explicit-implicit solvent model (dark blue). Structures presented are representative for the combined explicit-implicit solvent model



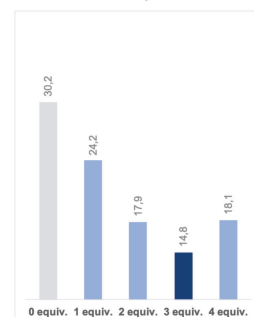
## b) Calculated free energy for transition states and intermediates

Evaluation of the influence of three different alcohols.

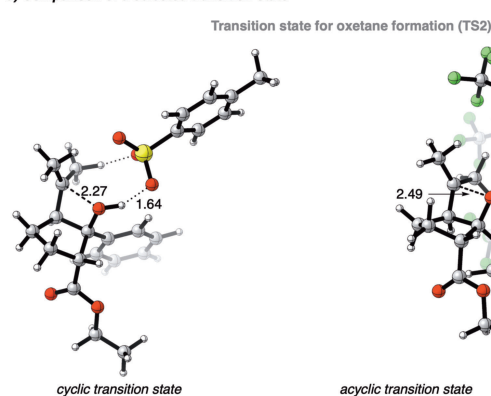


## c) Influence of the stoichiometry

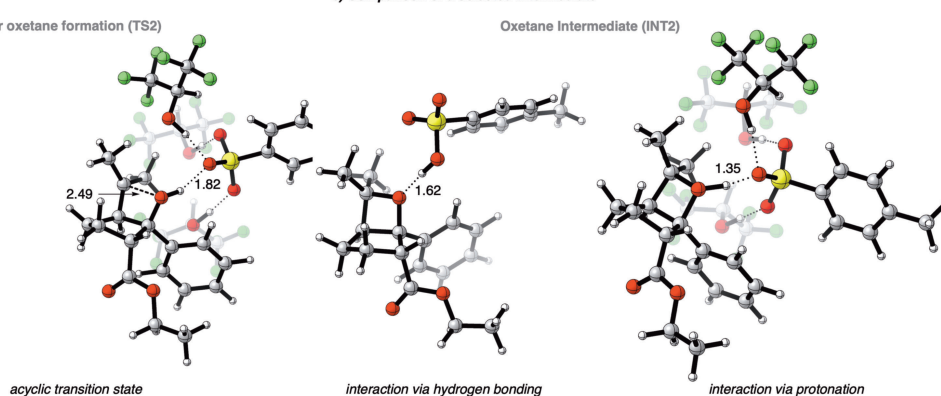
Influence of number of explicit HFIP molecules



## d) Comparison of a selected transition state



## e) Comparison of a selected intermediate



**Scheme 2.** Theoretical calculations on the pTSA-catalyzed COM reaction and the influence of HFIP hydrogen-bond networks. Level of theory: B3LYP-D3BJ/def2-tzvp (SMD = HFIP)/B3LYP/def2-svp.

product **2a**. Each of these four elementary reaction steps is catalyzed by pTSA, i.e. i) activation of the carbonyl group in the C–C bond-formation step, ii) and iii) hydrogen-bond interactions during ring-closing and ring-opening of the oxetane and iv) activation of the carbonyl group that leads to cleavage of the acetone by-product and release of the COM product, respectively.

While the reaction pathway is not altered by the introduction of the hydrogen-bond network and with/with-

out the hydrogen-bond network the oxetane ring formation remains the rate-determining step. The hydrogen-bond network has however a significant influence on the activation free energy along the path of the COM reaction (Scheme 2a, grey vs. blue profile). For instance, the barrier of the initial C–C bond formation is reduced from 23.9 to 12.9 kcal mol<sup>-1</sup> in the presence of 3 molecules of HFIP (Scheme 2a, **TS1**). Similarly, the introduction of 3 molecules of HFIP leads to a significant reduction of the activation free energy of the

oxetane formation, which was identified as rate-determining step with an activation free energy of  $30.2 \text{ kcal mol}^{-1}$  without HFIP and  $14.8 \text{ kcal mol}^{-1}$  in the presence of 3 molecules of HFIP, respectively. In the second stage of the reaction, the oxetane intermediate **INT2** is ring-opened in the presence of the pTSA catalyst. The introduction of additional molecules of HFIP similarly leads to a marked reduction of the activation free energies, e.g. from  $25.3$  to  $13.9 \text{ kcal mol}^{-1}$  for the formation of the carbocation intermediate **INT3** upon introduction of three explicit molecules of HFIP. Thus, the formation of a hydrogen-bond network of **1a**, pTSA and three molecules of HFIP leads to a significant lowering of the activation free energy and renders the room temperature COM reactions with simple Brønsted acids possible. These results agree well with our experimental kinetic studies (Figure 1).

In the course of these studies, we also performed the analysis of non-covalent interactions (for details, see Figure S22 in the computational Supporting Information), energy decomposition (for details, see Table S1 in the computational Supporting Information) and potential solvent–substrate interaction of HFIP with other Lewis-basic sites of **1a**. Although, such HFIP–substrate interactions were found possible, their influence on the course of the reaction was not taken further into account. These very weak HFIP–substrate interactions are in equilibrium with unbound HFIP and free substrate molecules (see page S8 in the experimental Supporting Information for HFIP–substrate complexation study) and thus would not affect the course of the reaction. For example, the hydrogen-bonding of **1a** with the pTSA–HFIP<sub>3</sub> catalyst is favored by  $1.4 \text{ kcal mol}^{-1}$  over the non-bonding situation. The respective interaction for acetone is favored by  $1.5 \text{ kcal mol}^{-1}$ —thus an equilibrium between bound and free catalyst will be present in solution and can drive the reaction to product formation (please see Figure S15 in the computational Supporting Information for further details).

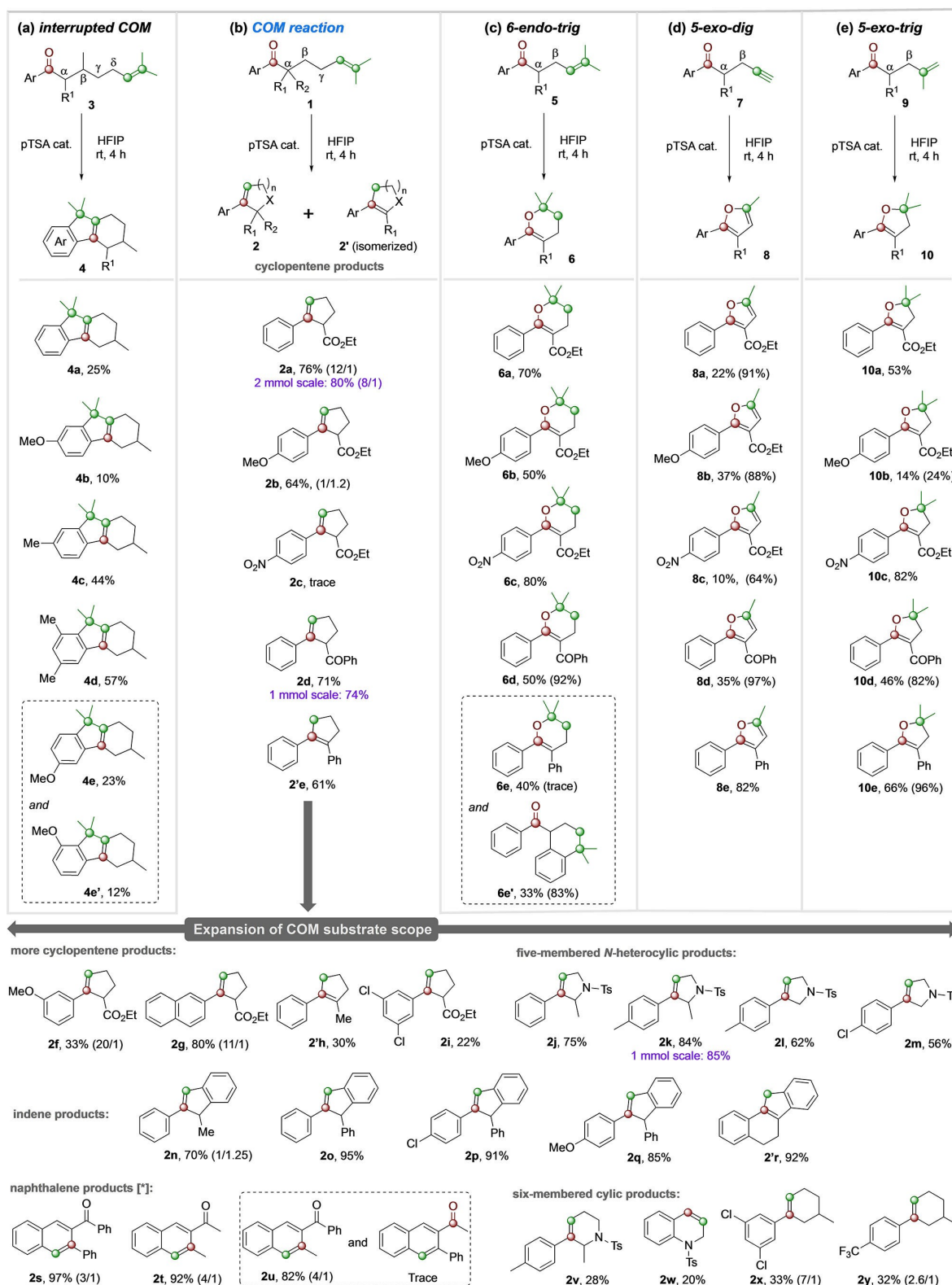
Next, we performed a closer examination of the influence of the hydrogen-bond network with different alcohol solvents on the activation of the pTSA catalyst (Scheme 2b). First, we examined *i*PrOH as a close analogue of HFIP to model the influence of a weak hydrogen-bond donor (Scheme 2b, grey). In this case relatively high activation free energies were observed, which are comparable to calculations with an implicit solvent (cf. Scheme 2a). The activation free energy of the rate-determining step was calculated with  $28.4 \text{ kcal mol}^{-1}$ , which is too high to proceed at room temperature with reasonable efficiency. Next, we examined trifluoroethanol as a model for an increased ability to form hydrogen-bond networks (Scheme 2b, light blue). In comparison to *i*PrOH, the hydrogen-bond network of solvent and catalyst results in a significant reduction of the activation free energy of all transition states. However, only in the case of the strong hydrogen-bond donor HFIP (Scheme 2a and b, dark blue), the activation free energies for all reaction steps are significantly reduced to enable for efficient COM reaction. Further calculations concerned the analysis of the influence of the stoichiometry of HFIP and catalyst. This analysis reveals that three molecules of HFIP

form an optimal hydrogen-bond network and allow for the COM reaction to proceed under mild conditions (Scheme 2c), which can be attributed to the presence of three oxygen atoms in pTSA that are required for hydrogen-bonding to three molecules of HFIP (Scheme 2d, e). These calculations now show that HFIP engages in the formation of hydrogen-bonding interactions with the pTSA catalyst that results in an encapsulation of the catalyst within a hydrogen-bond network. This hydrogen-bond network thus alters properties of the pTSA catalyst and consequently the transition-state energies for each step.

The optimized conditions developed in Table 1 were then applied to a range of intramolecular COM substrates (Scheme 3b).  $\alpha$ -Substituted ketoester substrates reacted smoothly to form their corresponding cyclopentene products in moderate to high yields (**2a–i**). For some substrates, the isomerized cyclopentenenes were obtained as major products (**2e** and **2h**), which was expected in this Brønsted acidic environment. Five-membered *N*-heterocyclic products could also be formed by this method in good to high yields, although the reactions on non  $\alpha$ -substituted systems (**2l, m**) were less efficient than those of  $\alpha$ -substituted ones (**2j, k**). These reactions also worked well when scaled up to 1–2 mmol scale, giving similar product yields (**2a, 2d** and **2k**). The reaction worked particularly well to form indene derivatives (**2n–q** and **2r**), which can be attributed to the stability of the conjugate indene ring that formed (Scheme 3). Similarly, a range of naphthalene products (**2s–u**) could be efficiently synthesized using our developed conditions. There were also competing carbonyl–ene side processes in these reactions. The application of these conditions to the formation of six-membered carbocyclic or *N*-heterocyclic products only led to moderate reaction outcomes (**2v–y**, Scheme 3b).

As discussed earlier, the directed Brønsted acid catalyzed COM reaction in homogeneous conditions is often problematic in that several side processes such as carbonyl–ene, Prins or interrupted carbonyl–olefin metathesis reactions can occur.<sup>[26]</sup> As our pTSA/HFIP catalytic system marked the first time COM reactions can be carried out in this manner without much of those issues, we would like to expand the work to investigate the scope of its catalytic activity on analogous cyclization reactions. We decided to select a series of aromatic ketones with an unsaturated side chain (**1, 3, 5, 7, 9** Scheme 3) and subjected them to the pTSA/HFIP catalytic conditions. The  $\epsilon,\zeta$ -unsaturated ketone substrates in Scheme 3a were based on Schindler's interrupted COM reaction substrates.<sup>[26a]</sup> They have unsaturated side chains with one more carbon than the COM  $\delta,\epsilon$ -unsaturated ketone substrates in Scheme 3b. The  $\gamma,\delta$ -unsaturated ketone substrates in Scheme 3c can be considered one  $\text{CH}_2$  truncated versions of the COM substrates.<sup>[29]</sup> The alkenyl and alkynyl<sup>[30]</sup> keto substrates in Scheme 3d and e bear slightly different unsaturated side chains but can be considered synthetic equivalents of the ones in Scheme 3c.

Most of these tested substrates cyclized under our pTSA/HFIP catalytic conditions to give the corresponding products (**2, 4, 6, 8**, Scheme 3) in moderate to high yields within four hours at ambient temperature. Some cyclization



**Scheme 3.** Substrate scope of COM reaction and analogous cyclization reactions under pTSA/HFIP catalytic conditions: (unless otherwise specified) substrate (0.2 mmol), pTSA (10 mol%), HFIP (100  $\mu$ L) at RT for 4 h.<sup>[27]</sup> For the formation of product **4**, reactions were carried out in PhCl/HFIP (1.8 mL/0.2 mL) for 18 h.<sup>[27]</sup> Yields in parentheses are of isolated products. Yields in brackets are of reactions carried out at 50 °C. Ratio in parentheses are of products **2** to **2'**. [\*] COM products were produced in inseparable mixtures with carbonyl-ene products, ratio of COM/carbonyl-ene products are quoted in parentheses.<sup>[27]</sup>

processes required to be carried out at 50°C to afford satisfactory outcomes, as indicated by product yields in parentheses. It is interesting to see that an electron-donating substituent such as OMe or an electron-withdrawing substituent such as NO<sub>2</sub> can have completely opposite effects on the outcomes of these 6-*endo-trig* (Scheme 3c), 5-*exo-dig* (Scheme 3d) and 5-*exo-trig* (Scheme 3e) cyclization reactions.

To rationalize this unexpected outcome, we analyzed the influence of electronic effects on the transition states of these cyclization reactions. The theoretical analysis reveals an early transition state without participation of the carbonyl group in the case of 6-*endo-trig* and 5-*exo-trig* cyclizations, which leads to a cyclic intermediate for both electron-donating and electron-withdrawing substituents. The subsequent deprotonation step is however dependent on the electronic properties of this substituent, which results in the formation of the thermodynamically preferred product in the case of an electron-withdrawing nitro group. In contrast, this deprotonation step is energetically disfavored in the case of an electron-donating OMe group and can thus reason the observed experimental outcome (please see Figures S16–S19 in the computational Supporting Information for further details). In contrast, the 5-*exo-dig* cyclization occurs via a late transition state with the participation of the pendant carbonyl group, which reasons a significant influence of the electronic properties on the initial cyclization step and can thus rationalize the reduced reaction yield (please see Figure S20, S21 in the computational Supporting Information for further details).

When there was an aromatic substituent at the alpha position, the 6-*endo-trig* cyclization was not the only predominant reaction pathway (Scheme 3c, product **6e/6e'**). The substrate could also cyclize in a Friedel–Crafts alkylation fashion to form tetrahydronaphthalene product **6e'**, which became the single major product at elevated temperature. This reaction pathway<sup>[31]</sup> is directly relevant to the formation of products **4** in Scheme 3a, where presumably the carbocation intermediate from a COM process also underwent Friedel–Crafts alkylation reaction onto the adjacent aromatic ring to form the tricyclic system.<sup>[26a]</sup> Such interrupted COM reaction is possible for this type of substrate but not the typical COM substrate (Scheme 3b), which can be attributed to the conformational arrangement of the initially formed six-membered ring. The efficiency of the interrupted COM reaction mediated by our pTSA/HFIP, albeit not fully optimized, was slightly lower than that of the earlier study with TfOH catalyst by Schindler and co-workers.<sup>[26a]</sup> It posed the question of how different does HFIP make those pTSA-catalyzed reactions in Scheme 3 in comparison to a normal organic solvent. Furthermore, would the super Brønsted acidic TfOH overcome the need for the “magical effect” of HFIP to efficiently promote those cyclization reactions in a normal organic solvent?

Thus, we decided to carry out a comparative study where we performed two of each type of the 6-*endo-trig* cyclization, the COM reactions and the interrupted COM reactions in different sets of conditions with pTSA/DCE, pTSA/HFIP, TfOH/DCE and TfOH/HFIP (Table 2, for further details on

these studies and also the reaction performances on the 5-*exo-trig*, 5-*exo-dig* cyclizations, see page S70 in the experimental Supporting Information). Interestingly, we observed clear differences in reaction efficiency. In general, pTSA in DCE was inefficient for all three types of reaction. pTSA/HFIP system proved to be a lot more superior than TfOH/DCE in the COM cyclization (products **2a** and **2e**). For the 6-*endo-trig* cyclization (products **6a** and **6e/6e'**), TfOH/DCE was slightly inferior to pTSA/HFIP, especially when it came to the formation of Friedel–Crafts type product **6e'** at elevated temperature. Similar catalyst/solvent-reactivity relationship was observed for the interrupted COM products (**4a** and **4d**). Surprisingly, with electron deficient substrates, the COM reactions (**2i** and **2z**) did not work well in all conditions; the interrupted COM substrates actually led to the formation of six-membered ring normal COM products (**4x/2x** and **4y/2y**); while the 6-*endo-trig* reactions (**6x** and **6y**) work well under all conditions. TfOH/HFIP system worked better than TfOH/DCE but not much better than pTSA/HFIP. These results once again confirmed the very important role of HFIP solvent and formation of hydrogen-bond networks in these Brønsted acid catalyzed reactions, in that it reduces the gap of efficiency between two Brønsted acids with very different  $pK_a$ .

The above comparative study on the influence of the carbon skeleton on the reaction outcome encouraged us to further examine and rationalize this intriguing divergent reactivity. It is of particular interest to understand current limitations<sup>[13]</sup> in carbonyl olefin metathesis ring-closing reactions and the specific reactivity for the preferential formation of cyclopentenes. The corresponding cyclobutenes or cyclohexenes are not favored products from COM cyclization and highly specialized catalysts are required in scarce number of reports for the latter.<sup>[12f,18b]</sup> We therefore carried out computational studies on the COM reaction pathway and all other reaction pathways observed for different chain length of the alkenyl carbon skeleton (Scheme 4). The analysis of the first reaction step showed a distinct effect of the carbon chain length on the activation free energy for C–C bond formation (**TS1**). This step is energetically favored for the hexene (**1**,  $n=2$ ) and heptene (**3**,  $n=3$ ) substrates, while being energetically highly unfavorable for the shorter pentene derivative (**5**,  $n=1$ ) due to the high ring strain of the putative 1-oxo-bicyclo-[2.2.0]-hexane intermediate (**TS1-1**) (Scheme 4, dark blue). Instead, **5** preferentially undergoes a 6-*endo dig* cyclization reaction via **TS5** to give pyrane **6a** (Scheme 4, green). The analysis of similar cyclization pathways for hexene (**1**,  $n=2$ ) and heptene (**3**,  $n=3$ ) substrates showed that such cyclization is indeed possible, yet disfavored due to the formation of larger ring systems and transannular interactions within such ring systems.<sup>[32]</sup>

The second reaction step then rationalizes for the divergent reactivity of the hexene (**1**,  $n=2$ ) and heptene (**3**,  $n=3$ ) substrates. Both substrates can potentially undergo a proton migration reaction<sup>[33]</sup> via the bicyclic transition state **TS6**, which results in the product of a classic ene reaction (**INT4**) via a stepwise reaction mechanism. Following the stepwise ene reaction, the tricyclic reaction product **6a** (Scheme 4, light

**Table 2:** Comparison of reactions using two different catalytic systems: pTSA/HFIP and TfOH/DCE.<sup>[a]</sup>

	A		B			
	<b>interrupted COM</b>		<b>COM reaction</b>		<b>6-endo-trig</b>	
	3	4	1	2	5	
	cat. solvent		cat. solvent		cat. solvent	
	4		2		6	
Product		<b>4a</b>		<b>2a</b>		<b>6a</b>
pTSA/DCE	ND		ND (10% <sup>[b]</sup> )		traces	
pTSA/HFIP	30%		78% <sup>[b]</sup>		73%	
TfOH/DCE	25%		36% <sup>[b]</sup> (54% <sup>[b]</sup> )		67%	
TfOH/HFIP	10%		66% <sup>[b]</sup>		82%	
Product		<b>4d</b>		<b>2e'</b>		<b>6e</b> and <b>6e'</b>
pTSA/DCE	ND		ND (ND)		<b>6e</b> : traces (38%); <b>6e'</b> : ND (traces)	
pTSA/HFIP	58%		77% <sup>[b]</sup>		<b>6e</b> : 42% (trace); <b>6e'</b> : 35% (83%)	
TfOH/DCE	37%		24% <sup>[b]</sup> (64% <sup>[b]</sup> )		<b>6e</b> : 45% (7%); <b>6e'</b> : traces (28%)	
TfOH/HFIP	65%		82% <sup>[b]</sup>		<b>6e</b> : 50% (traces); <b>6e'</b> : 21% (63%)	
Product		<b>4x</b>		<b>2x</b>		<b>2i</b>
pTSA/DCE	<b>4x</b> : ND; <b>2x</b> : ND		ND		ND	
pTSA/HFIP	<b>4x</b> : not formed; <b>2x</b> : 34% (7:1)		22%		78%	
TfOH/DCE	only traces of both <b>4x</b> and <b>2x</b>		traces		79%	
TfOH/HFIP	<b>4x</b> : not formed; <b>2x</b> : 12%		12%		81%	
Product		<b>4y</b>		<b>2y</b>		<b>2z</b>
pTSA/DCE	<b>4x</b> : ND; <b>2x</b> : ND		no product		ND	
pTSA/HFIP	<b>4y</b> : not formed; <b>2y</b> : 32% (7:1)		no product		81%	
TfOH/DCE	only traces of both <b>4y</b> and <b>2y</b>		no product		81%	
TfOH/HFIP	<b>4y</b> : not formed; <b>2y</b> : 9%		no product		83%	

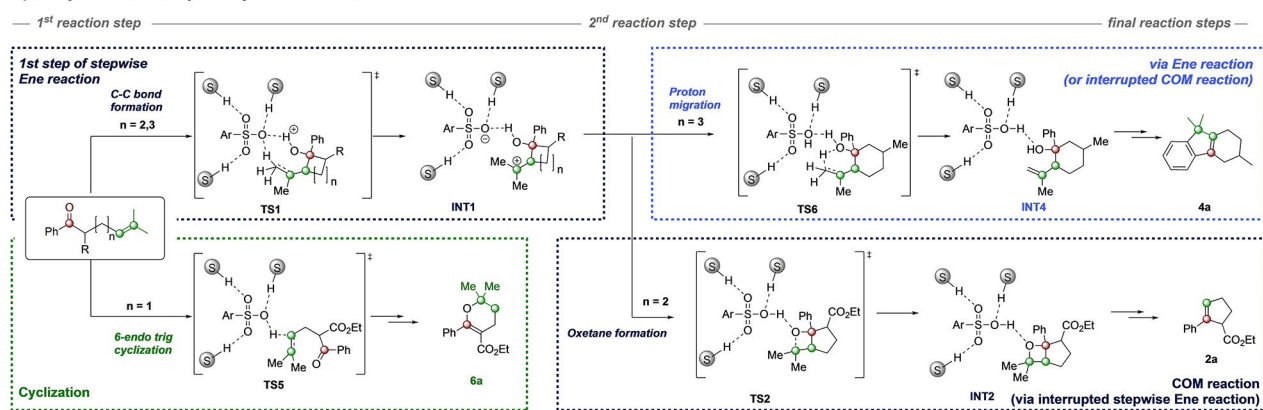
[a] Reaction conditions: Substrate (0.2 mmol), pTSA or TfOH (10 mol%), HFIP or DCE (100  $\mu$ L) at RT for 4 h. Yields were determined by <sup>1</sup>H NMR integration using mesitylene as an internal standard. Yields in parentheses are of reactions carried out at 50 °C. [b] Overall yields of two olefin isomers **2/2'**.

blue) is formed, which is often referred to as the product of an interrupted COM reaction. The interruption of the ene reaction pathway however, allows the formation of the bicyclic oxetane intermediate (**INT2**) via transition state **TS2** that ultimately leads to COM reaction (Scheme 4, dark blue). Thus,

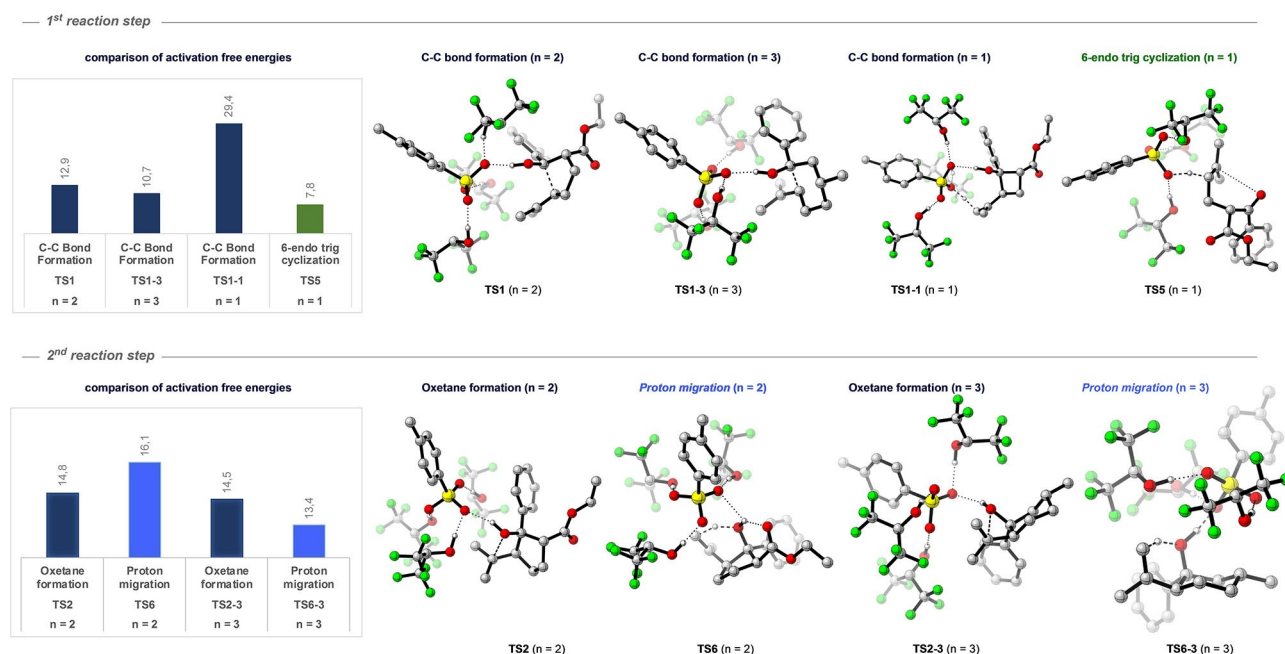
the initial steps of a COM reaction can also be regarded as an interrupted stepwise ene reaction. This pathway is favored only in the case of the hexene derivative **1**, as the formation of bicyclic oxetane intermediate **INT2** is conformationally accessible due to the envelope conformation of 5-membered rings.



## a) Analysis of reaction pathways for different side chains



## b) Comparison of activation free energy and transition state structures for different chain length for key reaction steps



Scheme 4. Comparison of the influence of the alkenyl chain length on the reaction outcomes.

In the case of heptenes (**3**), this pathway cannot be accessed as the six-membered ring needs to adopt an unfavorable twist boat conformation. Small differences in the energy of transition states that result from conformational restriction of bicyclic transition states and/or intermediates thus open a divergent reactivity that can lead to cyclization, carbonyl olefin metathesis or Ene reaction.

## Conclusion

In summary, we report on a combined experimental and computational study on the activation of catalysts by hydrogen-bonding interaction. We show that HFIP can act as a hydrogen-bond donor to enhance the catalytic efficiency of simple Brønsted acid catalysts by stabilization of all transition states and intermediates along the reaction pathway. This mode of activation could successfully be employed to allow for

a novel and practical method for the direct Brønsted acid catalyzed carbonyl-olefin metathesis reaction. Interesting insights into the effect of the alkenyl moiety chain length on the reaction outcomes were also revealed, which give the rationalization for the current ring-size limitation of COM cyclization reaction products. These results will not only advance the catalytic scope of the COM reaction further into homogeneous Brønsted acid catalysis but also pave the way for further investigations and applications of hydrogen-bonding network assisted catalysis in organic synthesis.

## Acknowledgements

This work was funded by the Australian Research Council (grant FT180100260 to T.V.N. and DP200100063 to T.V.N. and R.M.K.). C.P. thanks China Scholarship Council for a PhD scholarship. Open access publishing facilitated by Uni-

versity of New South Wales, as part of the Wiley - University of New South Wales agreement via the Council of Australian University Librarians.

### Conflict of Interest

The authors declare no conflict of interest.

### Data Availability Statement

The data that support the findings of this study are available in the Supporting Information of this article.

**Keywords:** Brønsted Acid Catalysis · Carbonyl-Olefin Metathesis · HFIP · Hydrogen-Bonding · Perfluorinated Solvent

- [1] E. V. Anslyn, D. A. Dougherty in *Modern Physical Organic Chemistry*, University Science Books, Sausalito, **2006**, pp. 145–204.
- [2] G. A. Jeffrey, W. Saenger in *Hydrogen Bonding in Biological Structures*, Springer, Berlin, Heidelberg, **1991**, pp. 167–422.
- [3] J. Meeuwissen, J. N. H. Reek, *Nat. Chem.* **2010**, *2*, 615–621.
- [4] a) D. Herschlag, M. M. Pinney, *Biochemistry* **2018**, *57*, 3338–3352; b) L. J. Karas, C.-H. Wu, R. Das, J. I.-C. Wu, *WIREs Comput. Mol. Sci.* **2020**, *10*, e1477; c) S. Dai, L.-M. Funk, F. R. von Pappenheim, V. Sautner, M. Paulikat, B. Schröder, J. Uranga, R. A. Mata, K. Tittmann, *Nature* **2019**, *573*, 609–613.
- [5] a) P. R. Schreiner, *Chem. Soc. Rev.* **2003**, *32*, 289–296; b) R. R. Knowles, E. N. Jacobsen, *Proc. Natl. Acad. Sci. USA* **2010**, *107*, 20678–20685.
- [6] S. E. Reisman, A. G. Doyle, E. N. Jacobsen, *J. Am. Chem. Soc.* **2008**, *130*, 7198–7199.
- [7] I. Takahashi, T. Fujita, N. Shoji, J. Ichikawa, *Chem. Commun.* **2019**, *55*, 9267–9270.
- [8] T. Kamitanaka, K. Morimoto, K. Tsuboshima, D. Koseki, H. Takamuro, T. Dohi, Y. Kita, *Angew. Chem. Int. Ed.* **2016**, *55*, 15535–15538; *Angew. Chem.* **2016**, *128*, 15764–15767.
- [9] P. R. Schreiner, *Science* **2010**, *327*, 965–966.
- [10] I. Colomer, A. E. R. Chamberlain, M. B. Haughey, T. J. Donohoe, *Nat. Rev. Chem.* **2017**, *1*, 0088.
- [11] V. Pozhydaiev, M. Power, V. Gandon, J. Moran, D. Lebœuf, *Chem. Commun.* **2020**, *56*, 11548–11564.
- [12] a) A. K. Griffith, C. M. Vanos, T. H. Lambert, *J. Am. Chem. Soc.* **2012**, *134*, 18581–18584; b) N. Veluru Ramesh, J. Bah, J. Franzén, *Eur. J. Org. Chem.* **2015**, 1834–1839; c) J. R. Ludwig, P. M. Zimmerman, J. B. Gianino, C. S. Schindler, *Nature* **2016**, *533*, 374–379; d) L. Ma, W. Li, H. Xi, X. Bai, E. Ma, X. Yan, Z. Li, *Angew. Chem. Int. Ed.* **2016**, *55*, 10410–10413; *Angew. Chem.* **2016**, *128*, 10566–10569; e) L. Pitzer, F. Sandfort, F. Strieth-Kalthoff, F. Glorius, *Angew. Chem. Int. Ed.* **2018**, *57*, 16219–16223; *Angew. Chem.* **2018**, *130*, 16453–16457; f) A. Djurovic, M. Vayer, Z. Li, R. Guillot, J.-P. Baltaze, V. Gandon, C. Bour, *Org. Lett.* **2019**, *21*, 8132–8137.
- [13] H. Albright, A. J. Davis, J. L. Gomez-Lopez, H. L. Vonesh, P. K. Quach, T. H. Lambert, C. S. Schindler, *Chem. Rev.* **2021**, *121*, 9359–9406.
- [14] a) A.-L. Lee, *Angew. Chem. Int. Ed.* **2013**, *52*, 4524–4525; *Angew. Chem.* **2013**, *125*, 4620–4621; b) E. T. Hennessy, E. N. Jacobsen, *Nat. Chem.* **2016**, *8*, 741–742; c) C. Saá, *Angew. Chem. Int. Ed.* **2016**, *55*, 10960–10961; *Angew. Chem.* **2016**, *128*, 11120–11121; d) J. R. Ludwig, C. S. Schindler, *Synlett* **2017**, *28*, 1501–1509; e) M. R. Becker, R. B. Watson, C. S. Schindler, *Chem. Soc. Rev.* **2018**, *47*, 7867–7881; f) L. Ravindar, R. Lekkala, K. P. Rakesh, A. M. Asiri, H. M. Marwani, H.-L. Qin, *Org. Chem. Front.* **2018**, *5*, 1381–1391; g) A. Das, S. Sarkar, B. Chakraborty, A. Kar, U. Jana, *Curr. Green Chem.* **2020**, *7*, 5–39.
- [15] a) J. R. Ludwig, S. Phan, C. C. McAtee, P. M. Zimmerman, J. J. Devery, C. S. Schindler, *J. Am. Chem. Soc.* **2017**, *139*, 10832–10842; b) C. C. McAtee, P. S. Riehl, C. S. Schindler, *J. Am. Chem. Soc.* **2017**, *139*, 2960–2963; c) E. J. Groso, A. N. Golonka, R. A. Harding, B. W. Alexander, T. M. Sodano, C. S. Schindler, *ACS Catal.* **2018**, *8*, 2006–2011; d) E. J. Groso, A. N. Golonka, R. A. Harding, B. W. Alexander, T. M. Sodano, C. S. Schindler, *ACS Catal.* **2018**, *8*, 2006–2011; e) H. Albright, P. S. Riehl, C. C. McAtee, J. P. Reid, J. R. Ludwig, L. A. Karp, P. M. Zimmerman, M. S. Sigman, C. S. Schindler, *J. Am. Chem. Soc.* **2019**, *141*, 1690–1700; f) P. S. Riehl, D. J. Nasrallah, C. S. Schindler, *Chem. Sci.* **2019**, *10*, 10267–10274; g) K. A. Rykaczewski, E. J. Groso, H. L. Vonesh, M. A. Gaviria, A. D. Richardson, T. E. Zehnder, C. S. Schindler, *Org. Lett.* **2020**, *22*, 2844–2848.
- [16] H. Albright, H. L. Vonesh, M. R. Becker, B. W. Alexander, J. R. Ludwig, R. A. Wiscons, C. S. Schindler, *Org. Lett.* **2018**, *20*, 4954–4958.
- [17] R. Wang, Y. Chen, M. Shu, W. Zhao, M. Tao, C. Du, X. Fu, A. Li, Z. Lin, *Chem. Eur. J.* **2020**, *26*, 1941–1946.
- [18] a) H. Albright, H. L. Vonesh, C. S. Schindler, *Org. Lett.* **2020**, *22*, 3155–3160; b) A. J. Davis, R. B. Watson, D. J. Nasrallah, J. L. Gomez-Lopez, C. S. Schindler, *Nat. Catal.* **2020**, *3*, 787–796.
- [19] a) X. Hong, Y. Liang, A. K. Griffith, T. H. Lambert, K. N. Houk, *Chem. Sci.* **2014**, *5*, 471–475; b) T. H. Lambert, *Synlett* **2019**, *30*, 1954–1965; c) Y. Zhang, J. Jermaks, S. N. MacMillan, T. H. Lambert, *ACS Catal.* **2019**, *9*, 9259–9264; d) J. Jermaks, P. K. Quach, Z. M. Seibel, J. Pomarole, T. H. Lambert, *Chem. Sci.* **2020**, *11*, 7884–7895; e) Y. Zhang, J. H. Sim, S. N. MacMillan, T. H. Lambert, *Org. Lett.* **2020**, *22*, 6026–6030.
- [20] S. Ni, J. Franzén, *Chem. Commun.* **2018**, *54*, 12982–12985.
- [21] U. P. N. Tran, G. Oss, D. P. Pace, J. Ho, T. V. Nguyen, *Chem. Sci.* **2018**, *9*, 5145–5151.
- [22] a) G. Oss, T. V. Nguyen, *Synlett* **2019**, *30*, 1966–1970; b) U. P. N. Tran, G. Oss, M. Breugst, E. Detmar, D. P. Pace, K. Liyanto, T. V. Nguyen, *ACS Catal.* **2019**, *9*, 912–919.
- [23] a) D. Roth, J. Stirn, D. W. Stephan, L. Greb, *J. Am. Chem. Soc.* **2021**, *143*, 15845–15851; b) T. Thorwart, D. Roth, L. Greb, *Chem. Eur. J.* **2021**, *27*, 10422–10427.
- [24] L. Catti, K. Tiefenbacher, *Angew. Chem. Int. Ed.* **2018**, *57*, 14589–14592; *Angew. Chem.* **2018**, *130*, 14797–14800.
- [25] M. Á. Rivero-Crespo, M. Tejada-Serrano, H. Pérez-Sánchez, J. P. Cerón-Carrasco, A. Leyva-Pérez, *Angew. Chem. Int. Ed.* **2020**, *59*, 3846–3849; *Angew. Chem.* **2020**, *132*, 3874–3877.
- [26] a) J. R. Ludwig, R. B. Watson, D. J. Nasrallah, J. B. Gianino, P. M. Zimmerman, R. A. Wiscons, C. S. Schindler, *Science* **2018**, *361*, 1363–1369; b) T. Malakar, P. M. Zimmerman, *J. Org. Chem.* **2021**, *86*, 3008–3016.
- [27] See the experimental Supporting Information for more details.
- [28] G.-X. Li, C. A. Morales-Rivera, F. Gao, Y. Wang, G. He, P. Liu, G. Chen, *Chem. Sci.* **2017**, *8*, 7180–7185.
- [29] R. B. Watson, A. N. Golonka, C. S. Schindler, *Org. Lett.* **2016**, *18*, 1310–1313.
- [30] A. N. Golonka, C. S. Schindler, *Tetrahedron* **2017**, *73*, 4109–4114.
- [31] R. B. Watson, C. S. Schindler, *Org. Lett.* **2018**, *20*, 68–71.
- [32] See the computational Supporting Information for more details.

[33] S. Jana, Z. Yang, F. Li, C. Empel, J. Ho, R. M. Koenigs,  
*Angew. Chem. Int. Ed.* **2020**, *59*, 5562–5566; *Angew. Chem.*  
**2020**, *132*, 5608–5613.

Manuscript received: December 20, 2021  
Accepted manuscript online: January 5, 2022  
Version of record online: February 10, 2022

---